Solution Structure of the PABC Domain from Wheat Poly (A)-Binding Protein: An Insight into RNA Metabolic and Translational Control in Plants†

Nadeem Siddiqui,‡ Michael J. Osborne,‡ Daniel R. Gallie,§ and Kalle Gehring*,‡

Department of Biochemistry, McGill University, 3655 Promenade Sir William Osler, QC H3G-1Y6, Canada, and Department of Biochemistry, University of California at Riverside, California 92521

Received September 24, 2006; Revised Manuscript Received December 29, 2006

ABSTRACT: In animals, the PABC domain from poly (A)-binding protein recruits proteins containing a specific interacting motif (PAM-2) to the mRNP complex. These proteins include Paip1, Paip2, and eukaryotic release factor 3 (eRF3), all of which regulate PABP function in translation. The following reports the solution structure of PABC from *Triticum avestium* (wheat) poly (A)-binding protein determined by NMR spectroscopy. Wheat PABC (wPABC) is an α-helical protein domain, which displays a fold highly similar to the human PABC domain and contains a PAM-2 peptide binding site. Through a bioinformatics search, several plant proteins containing a PAM-2 site were identified including the early response to dehydration protein (ERD-15), which was previously shown to regulate PABP-dependent translation. The plant PAM-2 proteins contain a variety of conserved sequences including a PABP-interacting 1 motif (PAM-1), RNA binding domains, an SMR endonuclease domain, and a poly (A)-nuclease regulatory domain, all of which suggest a function in either translation or mRNA metabolism. The proteins identified are well conserved throughout plant species but have no sequence homologues in metazoans. We show that wPABC binds to the plant PAM-2 motif with high affinity through a conserved mechanism. Overall, our results suggest that plant species have evolved a distinct regulatory mechanism involving novel PABP binding partners.

The poly (A)-binding protein (PABPC1, here referred to as PABP[1]) is a ubiquitous RNA binding protein found in all eukaryotes. It is the major protein complexed with 3′ poly (A)-tails of eukaryotic mRNA. Over the past few years, considerable evidence describes PABP as a multifunctional protein involved in a diverse range of fundamental cellular processes, including mRNA metabolism, mRNA export, and protein synthesis (*1*, *2*). A general function for PABP is to protect mRNA from deadenylation, the rate-limiting step in mRNA decay, by binding to the 3′-poly (A)-tail and physically limiting the access of exoribonucleases. In yeast (*3*) and mammals (*4*), PABP can shuttle between the nucleus and cytoplasm and has different functions depending upon its location in the cell.

In the nucleus, *Saccharomyces cerivisiae* (yeast) PABP (yPABP) was implicated in multiple steps involving poly (A)-processing of the 3′-end of nascent mRNA. This includes association with cleavage polyadenylation factors (CFI), which together with poly (A)-polymerase (PAP), are involved in poly (A)-synthesis (*5*, *6*). During the later steps, the association of yPABP with poly (A)-nuclease (PAN) (*7*) is necessary for trimming the poly (A)-tail to a length appropriate for efficient mRNA export. The requirement for PABP for trimming of the 3′-tail and interaction of the mRNA with export factors establishes yPABP's importance as a mediator of mRNA biogenesis and export (*8*, *9*). Recent work has demonstrated that in mammalian cells, PABP associates with the poly (A)-tail of unspliced pre-mRNA, co-immunopurifies with PAP, and remains on the transcript during the pioneer round of translation (related to nonsense-mediated decay) (*10*). In this context, mammalian PABP was suggested to be involved in pre-mRNA processing, stability, and quality control. The nuclear function of PABP in plants has not been as clearly characterized. However, cross-species complementation studies of yeast PABP null mutants show that *Arabidopsis thaliana* PAB2 (*11*), PAB3 (*12*), and PAB5 (*13*) can partially restore poly (A)-length control in a poly (A)-nuclease dependent manner. In these studies, PAB3 was present in the nucleus of the complimented yeast strain and promoted the rate of mRNA entry into the translated pool. This suggests an evolutionary conserved nuclear function of PABP in facilitating mRNA biogenesis and export (*14*).

The mechanism of protein synthesis and the macromolecules needed are very similar in yeast, animal, and plant cells (*15*). In the cytoplasm, PABP associates with both the mRNA poly (A)-tail and eukaryotic initiation factor 4G

† N.S. is a recipient of the McGill Graduate Study and Faculty of Medicine Internal Fellowship. K.G. is a Chercheur National of the Fonds de la recherche en santé Québec. This work was supported by Canadian Institute of Health Research Grant MOP-14219 to K.G and United States Department of Agriculture Grant (2003-35100-13375) to D.R.G.

* To whom correspondence should be addressed. Tel: (514)-398-7287. Fax: (514) 398-7384. E-mail: kalle.gehring@mcgill.ca.

‡ McGill University.

§ University of California at Riverside.

[1] Abbreviations: PABC, C-terminal domain of PABP; HSQC, heteronuclear single quantum correlation; hNOE, heteronuclear NOE; IF, initiation factor; ITC, isothermal titration calorimetry; mRNP, messenger ribonucleoprotein; NMR, nuclear magnetic resonance; NOE, nuclear Overhauser effect; PAM, PABC-interacting motif; PABP, poly (A)-binding protein; RRM, RNA recognition motif.

10.1021/bi061986d CCC: $37.00
Published on Web 03/15/2007

(eIF4G) (*16*), which along with eIF4E and eIF4A comprises the cap binding protein complex eIF4F. These associations stimulate eIF4A helicase activity (*17*), promote eIF4E to interact with the 5′-m7GpppX cap structure (*18*), and, along with eIF4B (*19*, *20*), increase PABP affinity for the poly (A)-tail on mRNA (*19*). The synergistic interactions between these proteins are thought to enhance translation by stabilizing the mRNP complex and promoting ribosomal recruitment (*21*). Simultaneous binding of the initiation factors to PABP loops the mRNA transcript and brings the mRNA 5′- and 3′-termini into close proximity (*22*). Circularization of mRNA further enhances translation by allowing terminating ribosomes to cycle on the same mRNA transcript (*23*). A notable difference in plant systems is the presence of an eIF4F isoform (eIFiso4F) (*24*). This complex, is composed of eIFiso4G, which also interacts with wheat PABP, and eIFiso4E, which can bind to 5′-capped mRNA (*19*). eIF4F and eIFiso4F isoforms have evolved to discriminate between nonstandard mRNA, that is, those containing a structured 5′-leader or multiple cistrons, and standard transcripts in plants, respectively (*25*).

The structure of PABP is highly conserved (*26*, *27*). It is a modular protein consisting of an N-terminal region with four RNA recognition motifs (RRMs) and a C-terminal region containing a peptide-binding module referred to as the PABC domain. Each RRM possess a canonical RNA binding fold of four stranded antiparallel β-sheets backed by two α-helices (*28*). The central two β-strands contact RNA while the α-helical face and RRM linker regions provide interaction sites for proteins such as eIF4B (*19*, *20*), eIF4G (*29*), DAZL (*30*), PABP-interacting proteins (Paip)-1 (*31*) and -2 (*32*), cleavage factor IA (*6*), Rna15p (*5*), and yeast export and import factors (*8*, *9*).

The PABC domain does not contact RNA, but serves as an additional binding surface for proteins. These include Paip-1, Paip-2, and eukaryotic release factor 3 (eRF3). Through its association with PABP, Paip-1 and Paip-2, stimulate (*33*) and down-regulate (*32*) protein translation, respectively. Both proteins contain two independent motifs that contact PABP, referred to as PABP-interacting motifs (PAM)-1 and -2 (*31*). The PAM-1 motif is an acidic sequence, which interacts with the N-terminal RRMs, whereas PAM-2 interacts with the PABC domain. Mammalian eRF3 contains a PAM-2 motif within its N-terminus and plays a role in ribosome release (*34*).

Over the past few years, structures of the PABC domain from human (*35*, *36*), *S. cerevisiae* (*27*), and *Trypanasoma cruzi* (*37*) have been solved. These domains are α-helical in nature and adopt a right-handed super coil fold. The structures of human PABC complexes with Paip-1 and Paip-2 show that the conserved 15-residue PAM-2 sequence is necessary and sufficient for binding (*38*). Although PABCs share high sequence similarity, at least 42% across species, structural differences exist most notably between human and yeast PABCs (*27*, *35*, *36*). These differences are responsible for the lower binding affinity of yPABC to PAM-2 sequences and suggest an alternative PABC binding motif in yeast (*27*).

Here, we report the solution structure of the PABC domain from wheat PABP and characterize its interaction with the plant PAM-2 sequence via NMR spectroscopy and isothermal calorimetry. Wheat PABC (wPABC) binds to the plant PAM-2 motif with high affinity and shows a structure and peptide recognition mechanism analogous to that of human PABC. A bioinformatic analysis of wheat and other plant sequence databases identified several novel proteins containing PAM-2 sequences with putative roles in either RNA metabolic or translational regulatory pathways. The plant proteins identified have no metazoan homologues but are found throughout plant species. These results suggest a conserved role for these proteins and implicate them as potential plant PABP binding partners.

EXPERIMENTAL PROCEDURES

Construct Design and Protein Sample Preparation. On the basis of previous studies with the human PABC domain (*35*), a primary sequence alignment between human (NCBI accession number: AAH15958) and wheat PABP (NCBI: AAB38974) indicated that the wheat PABC domain resides between residues Y535 and S651. Accordingly, this site was amplified by PCR and cloned into a glutathione *S*-transferase (GST)-fusion vector. This construct was produced as an unlabeled, ^{15}N, or $^{15}N/^{13}C$ isotopically labeled GST-fusion protein using the pGEX-2TK vector system (Amersham Biosciences). Protein expression was completed as described previously (*37*). The recombinant protein, wPABC1, was isolated by affinity chromatography using Glutathione Sepharose 4B resin (Amersham Biosciences). The fusion protein was eluted with the addition of 20 mM reduced glutathione in phosphate buffered saline (PBS) buffer at pH 7.1 and incubated overnight at 4 °C with thrombin protease (2 units/mg fusion protein, Amersham Biosciences). Further purification was done with an HPLC gel filtration column (Superdex 75HR 10/30, Amersham Biosciences) using 1× PBS at a flow rate of 0.5 mL/min to separate cleaved GST, thrombin protease, and other impurities from the target sample. Characterization by electrospray ionization (ESI) mass spectrometry confirmed the presence of a 13.7 kDa protein consisting of 129 residues, which included 12 additional N-terminal residues encoded by the expression vector. For NMR analysis, the purified sample was exchanged into an NMR buffer (50 mM $NaHPO_3$, 150 mM NaCl, 1 mM NaN_3, and 10% D_2O at pH 6.3) and concentrated by centrifugation (Amicon, MWCO 5000 kDa). The final protein concentrations in NMR samples were between ∼1 and 2 mM.

Our initial NMR experiments demonstrated that the wPABC1 construct contains unstructured regions at both the N- and C-termini (discussed in the Results section). Consequently, a second construct was made to include only the structured region. A PCR fragment corresponding to the structured region was amplified using the first construct as the template and oligos wPC-5′F: 5′-CACAGGGATCCCCAATTGGGGCATTGG-3′ and wPC-3R 5′-CACTCTCGAGTTAGGAAGAGATGAGGC-3′ (restriction sites are underlined). The product was cloned into the BamHI and XhoI sites of a pGEX-6P1 GST-fusion vector (Amersham Biosciences). The DNA sequence of the new construct wPABC2 residues (P552−S634) was verified by capillary electrophoresis-based sequencing using the Molecular Dynamics MegaBACE 500 system (Sheldon Biotech). The wPABC2 sample was prepared as described above, but PreScission protease (Amersham Biosciences) was used to cleave the recombinant protein from the GST-tag. Characterization of wPABC2 by ESI mass spectrometry confirmed

the presence of a 9.4 kDa protein consisting of 83 residues of wPABC2 and 5 additional N-terminal residues (GLPGS) encoded by the expression vector.

NMR Spectroscopy. All NMR experiments were acquired at 303 K using standard double and triple resonance techniques on ^{15}N- or ^{15}N,^{13}C-labeled samples (*39*). Experiments were done on Bruker DRX 600 MHz and Varian Unity Inova 800 MHz spectrometers. NMR spectra were processed using NMR Pipe/NMR Draw (*40*). Evaluation of spectra and manual assignments were completed with XEASY software (*41*). Sequential backbone and side chain assignments were determined using HNCACB and CBCA(CO)NH (*42*, *43*), 2D homonuclear TOCSY, and 3D ^{15}N-edited TOCSY. Distance restraints were derived from a 2D homonulcear NOESY and 3D ^{15}N-edited NOESY. ^{15}N-^{1}H hNOE experiments were acquired at 600 MHz in an interleaved manner with a recycle delay of 4 s (*44*). Values were measured by taking the ratio of peak intensities from experiments performed with and without ^{1}H presaturation. Saturation was achieved using a train of 120° pulses separated by 5 ms for a total irradiation time of 3 s.

Peptide Synthesis, Purification, and Titration Experiments by NMR. A region corresponding to a PAM-2 motif found in wheat (TIGR TC251957) 16-SLNPNAVEFVPSCLRS-31 was synthesized by Fmoc (*N*-(9-fluorenyl)methoxycarbonyl) solid-phase peptide synthesis and purified by reverse-phase chromatography on a Vydac C18 column (Sheldon Biotechnology Center). The composition and purity of the peptide was verified by ion-spray quadropole mass spectroscopy. NMR titrations were carried out by adding aliquots of unlabeled wPAM2 peptide to an ^{15}N-labeled wPABC sample until saturation was achieved. Signals were monitored by observing the change in chemical shifts of amide signals $(((\Delta^{1}\text{H ppm})^2 + (\Delta^{15}\text{N ppm} \times 0.2)^2)^{0.5})$ on HSQC spectra. HNCACB and CBCACONH experiments were carried out for backbone reassignment of wPABC in a 1:1 complex with PAM-2.

Isothermal Calorimetry (ITC) Measurements. Experiments were carried out on a MicroCal VP-ITC titration calorimeter using VPViewer software for data acquisition and instrument control (MicroCal, Inc., Northampton, MA). NMR buffer (as described above) was used for ITC experiments. A degassed sample of wPABC thermostated at the desired temperature (15 °C) and was stirred (310 rpm) in a reaction cell of 1.4 mL. Titrations were carried out using a 296 μL syringe filled with the peptide solution. Thirty-seven injections at 8 μL of peptide were added to the sample with a 5-min interval between injections. Heat transfer (μcal/s) was measured as a function of elapsed time. The experiments were performed with 50 μM wPABC solution in the cell and 500 μM peptide solution in the syringe to ensure a final peptide/protein molar ratio of 2:1 in the reaction cell. The binding constants and thermodynamic parameters were determined as described earlier (*38*).

Analysis of NMR Data and Structure Calculation. A set of unambiguous NOE restraints were extracted from the NOESY spectra and used in conjunction with dihedral angle restraints to generate a preliminary fold of wPABC using CNS 1.1 (*45*). The resulting structures were used as a model template for automated assignments by ARIA 1.1 (*46*). The final 3D structure of wPABC was calculated using standard molecular dynamics protocols in CNS 1.1 with a total set of 1148 restraints (Table 1) collected from the experiments described above. In the final round of calculations, only unambiguous restraints were used. CNS 1.1 was extended to incorporate dihedral angle and hydrogen bond restraints (*47*) for further refinement. Backbone dihedral angle restraints were obtained from the average values predicted by TALOS (*48*). Hydrogen bond restraints were determined from NOE patterns and expectations for helical residues. Fifteen structures were selected to represent the final ensemble on the basis of lowest energy and best fit to experimental restraints. PROCHECK-NMR was used to generate Ramachandran plots to check the protein's stereochemical geometry (*49*). The coordinates of wheat PABC have been deposited in the RCSB under PDB accession code 2DYD and the NMR assignments under BMRB accession number 15087.

Table 1: Structural Statistics for 15 Selected Conformers for Wheat PABC

Restraints Used for Structure Calculation		
intraresidue NOEs	($n = 0$)	541
sequential NOEs	($n = 1$)	242
medium range NOEs	($n = 2,3,4$)	122
long range NOEs	($n > 4$)	75
dihedral angle restraints		107
hydrogen bonds		61
total number of restraints		1148
Average rms Difference to Mean Structure (Å) for Residues N562−S626		
backbone atoms		0.465 ± 0.17
Average Energy Values (kcal mol^{-1})		
E_{total}		411.16 ± 5.28
E_{bond}		15.78 ± 1.02
E_{angle}		96.58 ± 2.50
$E_{improper}$		21.23 ± 0.50
E_{VdW}		134.14 ± 8.01
E_{NOE}		111.36 ± 11.56
$E_{dihedral}$		32.06 ± 6.62
Deviation from Idealized Covalent Geometry		
bonds (Å)		0.0035 ± 0.0001
angles (°)		0.5195 ± 0.0093
improper (°)		0.4756 ± 0.0104
rms Deviation from Experimental Data		
distance restraints (Å)		0.048 ± 0.004
dihedral angle restraints (°)		1.567 ± 0.169
Average Ramachandran Statistics for 20 Lowest Energy Structures		
residues in most favored region		80.8%
residues in additional allowed regions		15.1%
residues in generously allowed regions		4.1%
residues in disallowed regions		0.0%

Bioinformatics. Proteins containing the PAM-2 motif were identified through a basic local alignment search tool (BLAST) (*50*) at NCBI (http://www.ncbi.nlm.nih.gov/blast/) using the search for the "short nearly exact match" option. The input was a consensus PAM-2 sequence (-LNP-A-EFVP-), and the search limited to Viridiplantae. Default parameters were selected including a PAM30 matrix, which evaluates the quality of pairwise sequence alignment. Domain architecture of the identified proteins was found at the NCBI conserved domain database (*51*) and simple modular architecture research tools (SMART) (*52*). Wheat proteins were searched for in The Institute for Genomic Research (TIGR) databases using the BLAST search option (http://tigrblast.

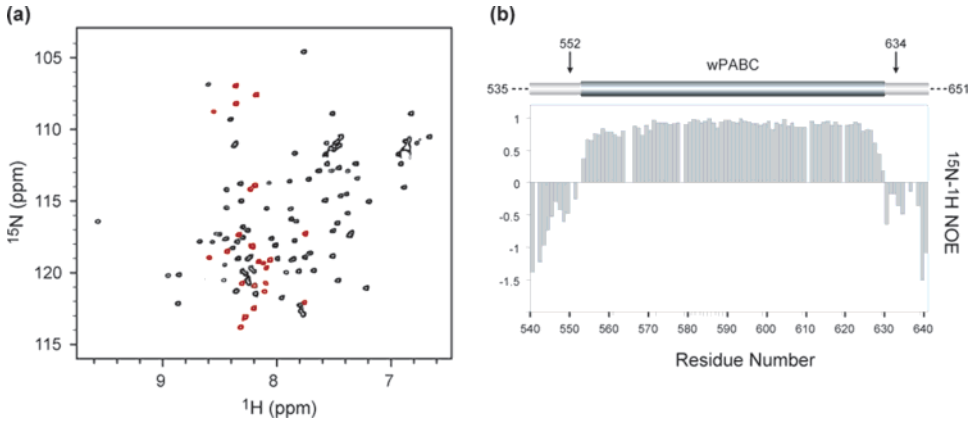

FIGURE 1: ^{15}N-^{1}H HSQC and identification of domain boundaries by heteronuclear NOE experiments. (a) ^{15}N-^{1}H HSQC of the C-terminal region of wheat PABP (residues Y535−S651). Signals from residues that were absent or negative in a ^{15}N-^{1}H heteronuclear NOE experiment are highlighted in red. These residues represent the unstructured regions outside of the domain. (b) Bar graph display of heteronuclear NOE values taken at 600 MHz as a function of residue number. Above the graph is a cartoon representation of the structured region in wheat PABC. The arrows indicate the regions where primers were designed to create the wPABC construct (residues P552−S634). All spectra were taken at 303 K.

tigr.org/tgi/). Multiple sequence alignments of proteins were computed using CLUSTAL W (or Boxshade) (*53*).

RESULTS

Sample Optimization. A ^{15}N-^{1}H HSQC experiment was performed on a uniformly ^{15}N-labeled sample corresponding to the C-terminal region of wheat PABP (NCBI AAB38974; Y535−S651). The HSQC spectrum for this construct (Figure 1a) displayed excellent signal dispersion and a total of 118 out of 129 amide−proton signals were observed. Chemical shifts were not observed for the 9 prolines or amides with significant overlap. HNCACB and CBCA(CO)NH experiments were performed on a ^{13}C/^{15}N labeled sample to obtain sequential backbone assignments. To acquire dynamic information and determine the unstructured regions of the protein, ^{1}H-^{15}N heteronuclear NOE experiments (hNOE) were performed. This experiment detects ^{15}N-^{1}H vector reorientational dynamics and is used to assess the motion of the protein backbone at the nano- to pico-second time scale. Negative hNOE values, which indicate regions of high flexibility, were found at the N-terminus (residues Y535−S551) and the C-terminus (residues H630−S651) (Figure 1b). Given this information, DNA primers were designed accordingly to eliminate the unstructured sections of the protein. The new construct corresponding to the structured region of wheat PABC (P552−S634) was prepared as an isotopically labeled recombinant protein for further structural studies by NMR spectroscopy and thermodynamic studies by isothermal titration calorimetry (ITC).

Sequence and Structure Comparison of Wheat PABC. Over 90% of backbone and side chain resonances were determined for ^{1}H and ^{15}N, and over 1100 restraints were used to calculate its structure (Table 1). The ensemble consisting of 15 least violated structures is shown in Figure 2a with the ribbon diagram in Figure 2b. This ensemble has a backbone root-mean-square deviation (rmsd) of 0.465 ± 0.17 Å for regions (N562−S626). The wPABC domain is a monomer principally consisting of four α-helices (residues E566−V580, Q587−L595, Q600−L606, D611−R625) that fold into a well-defined compact structure. Similar to *T. cruzi* PABC (*37*), there is a short N-terminal helix (A557−A559) that does not pack against the protein. However, the hNOE values of this region are only slightly lower than the rest of the protein, indicating that this region is ordered. Even though long-range NOEs could not be found within this region, it is plausible that this N-terminal helix could be packed, as observed in human PABC, within the full PABP protein in *T. cruzi* and wheat. Nevertheless, the 3D arrangement of the last four α-helices share structural similarities that are closer to that of *T. cruzi* and human than that of yPABC (Figure 2). The primary sequences of PABC domains are highly conserved across plant species. wPABC shares at minimum 54% sequence identity and 72% similarity with other plant PABCs (Figure 3). Importantly, the residues that build the hydrophobic core and account for the major stabilization force within the wPABC structure (such as L572, L576, V580, A588, V591, L596, L597, V603, L606, L613, and V617) are highly conserved throughout plant PABPs. From this observation, one can predict that the structures of the PABC domains from other plant PABPs will be similar to the domain from wheat.

In general, the largest variations within PABC structures across kingdoms are found at the N-terminus, which corresponds with the region with lowest sequence similarity (Figure 3). Only, hPABC contains an extra N-terminal α-helix that is tightly packed in the domain (*35*). The PABC domains from HYD and yeast PABP only contain four α-helices. The extra N-terminal helix in hPABC (NCBI NP002559; residues L544−A552) is dispensable as a shortened fragment and gives a ^{15}N-^{1}H HSQC spectrum similar to that of the full length domain (*27*). In addition, the mutant Δα1-hPABC (residues 554−636) can bind to Paip-2 with affinities comparable to that of the wild type domain (data not shown). PABC from HYD and TcPABP also has specificity and affinity to the PAM-2 motif similar to that of human PABP. Overall, this indicates that the last four helices are sufficient for sequence recognition. Furthermore, the extra N-terminal helix in animal, trypanosome, and plant species suggest a function independent of peptide recognition. Another notable structural difference in yeast PABC is a strong bend found exclusively within its C-terminal helix. This difference appears to be responsible for the significantly lower affinity for known PAM-2 sequences.

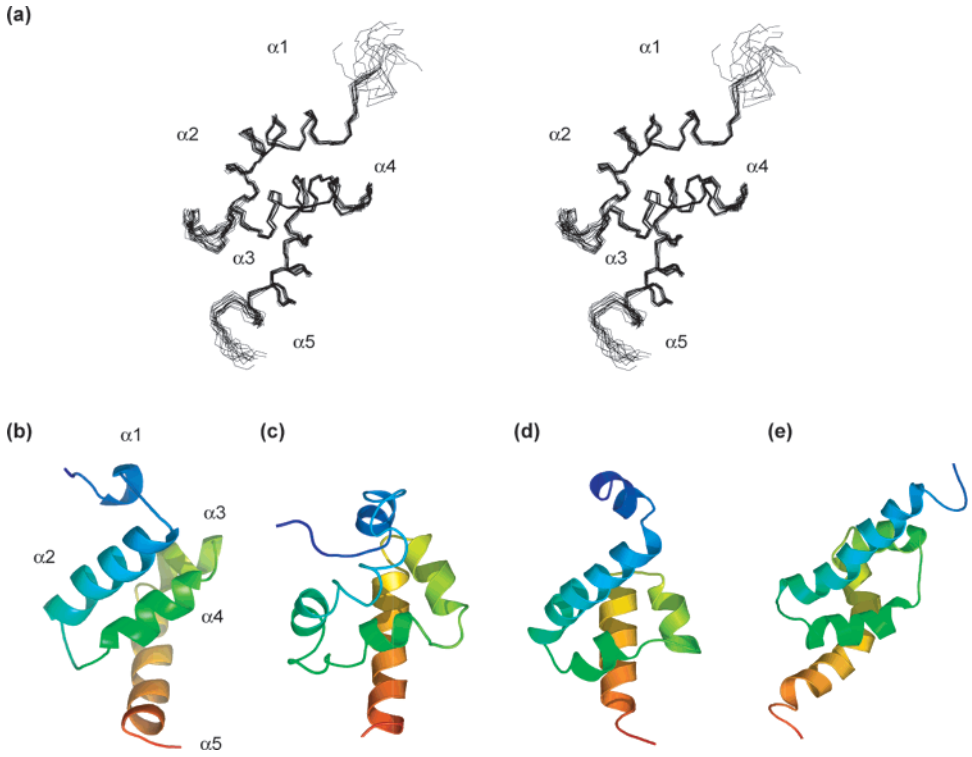

FIGURE 2: Comparison of PABCs from PABP. (a) Fifteen least violated wheat PABC conformers in cross-eyed stereo format. (b−e) Ribbon representation for the lowest energy structures of PABC from (b) wheat PABP (pdb 2DYD), (c) human PABP (PDB 1G9L), (d) *T. cruzi* PABP (PDB 1NMR), and (e) yeast PABP (PDB 1IFW). The rmsd overlays of secondary structural elements of wPABC onto the other structures are 1.53 Å for TcPABC, 1.55 Å for hPABC, and 1.62 Å for yPABC. Helices are colored from the N-terminal (blue) to C-terminal (red).

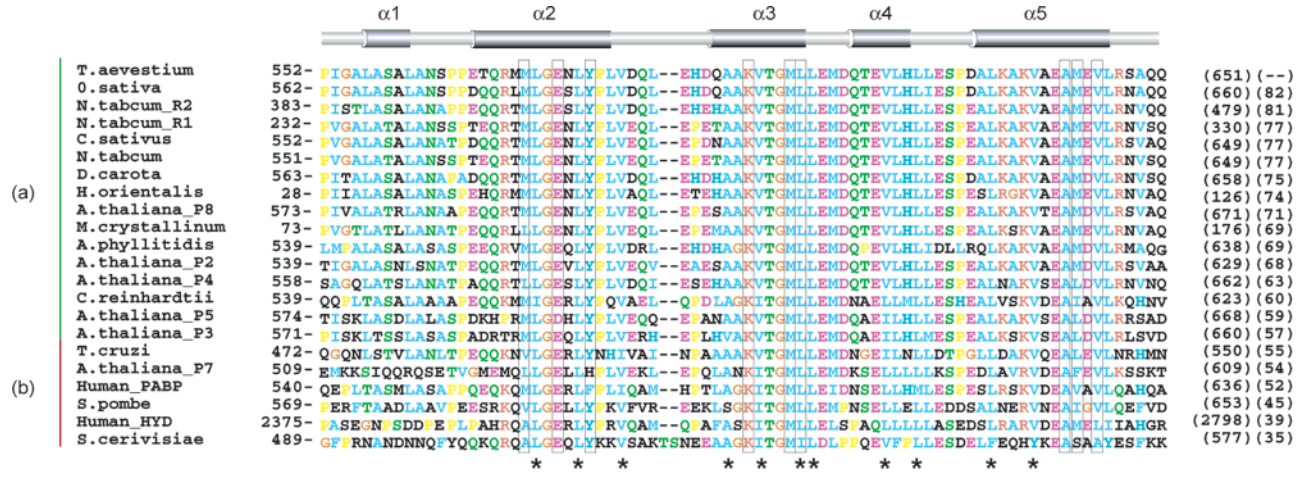

FIGURE 3: Sequence comparison of the PABC from plant PABPs. (a) Plant PABC sequences are shown next to the green bar, and (b) sequences from other species are next to the red bar. Comparison of PABCs derived from poly (A)-binding proteins from (NCBI accession numbers in parentheses) *T. aestivum* (AAB38974), *O. sativa* (XP_481529), *N. tabcum* PABP isoforms R2 (AAF66825) and R1 (AAF66824), *C. sativus* (AAF63202), *D. carota* (AAK30205), *H. orientalis (*AAT08650), *A. thaliana* PABP isoforms 2 (AAA61780), 3 (NP_173690), 4 (NP_179916), 5 (AAA61780), 7 (NP_181204), and 8 (NP_564554), *M. crystallinum (*AAB61594), *C..reinhardtii* (AAC39368), *T. cruzi* (AAC02538), human (AAH41863), *S. pombe* (CAB08762), and *S. cerivisiae* (P04147) and PABC from the hyperplastic disk gene/HYD (AAF88143). Highlighted residues show sequence conservation between PABCs. Above the alignment is a cartoon representation of the α-helices found in PABCs. The starting residue position within the protein is shown at the beginning of each sequence. The end of each sequence shows the total size of the protein followed by the percent identity with reference to wheat PABC. The asterisk denotes the residues that participate in building the protein's hydrophobic core. The residues that are boxed in indicate those that participate in peptide binding.

The PABC binding site in *S. cerevisiae* appears to be different from sequences in metazoans (*27*).

Isothermal Calorimetric Measurements and the Peptide Binding Interface of wPABC with a PAM-2 Peptide. A 16 residue peptide corresponding to a PAM-2 motif in one of the wheat proteins identified by bioinformatics analysis (*vida infra*) (Figure 4) was synthesized for binding studies with wPABC. Isothermal titration calorimetry (ITC) experiments were completed to determine the thermodynamic parameters for wPABC-PAM2 binding. The titration of wPABC with peptide resulted in negative deflections from the baseline, which is indicative of an exothermic reaction (Figure 5c). The heat of release allowed for measurements of the enthalpy, entropy, and Gibbs free energy of binding. The

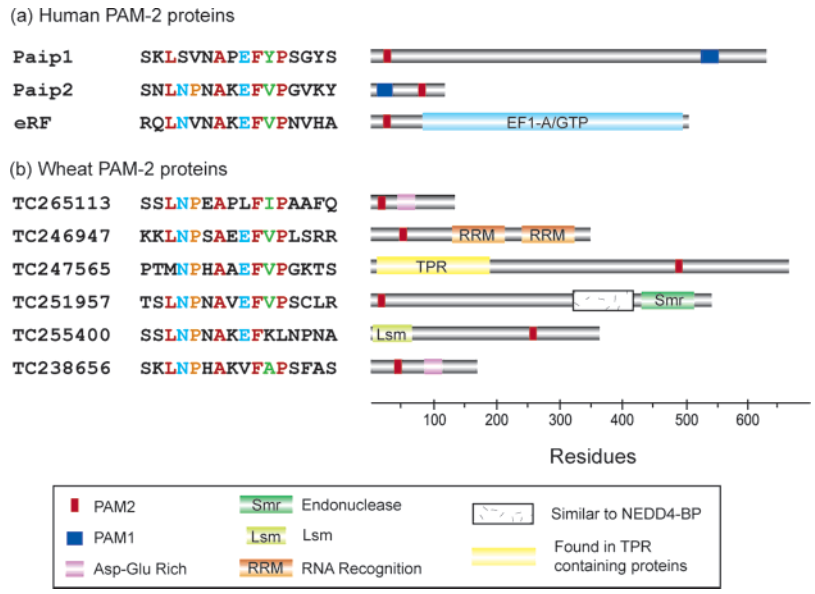

FIGURE 4: Identification of wheat proteins containing the PAM-2 site. (a) Human Paip-1 and Paip-2 both contain a stretch of acidic residues that interact with the N-terminal RRM region of PABP (referred to as PABP-interacting motif-1, PAM-1). Paip-1, Paip-2, and eukaryotic release factor 3 all contain a conserved PAM-2 site. RF3 also contains a GTPase site similar to elongation factor 1-α. (b) Wheat proteins containing a PAM-2 motif. These proteins contain an array of different modules, including acid-rich sequences, RNA recognition motifs, an Smr endonuclease domain, TPR, and an Lsm domain. The shaded box corresponds to regions that share similarities with the human BCL-3 protein/NEDD4BP.

interaction is dominated by favorable enthalpic effects ($\Delta H = -7.1$ kCal/mol), which give rise to heat release upon binding. The slightly positive entropy ($\Delta S = 0.174$ kCal K^{-1}/mol) indicates that desolvation effects most likely dominate conformational ordering upon complex formation. Assuming a 1:1 binding model, the ITC measurements yielded a K_d value of 3.0 μM, indicating a reasonably strong affinity between the peptide and protein. Our measured K_d and thermodynamic profile are comparable with previous binding studies observed between hPABC and peptides derived from human Paip-1, Paip-2, and RF3 (*38*). Because each of these proteins was demonstrated to interact with PABP *in vivo* (*31*, *32*, *54*), the measured affinities in the low micromolar range can be considered physiologically relevant.

The peptide binding site on wPABC was determined by NMR using chemical shift perturbation analysis. A ^{15}N labeled sample of wPABC was titrated with the unlabeled peptide, and residues showing chemical shift changes were monitored on a ^{15}N-^{1}H HSQC spectrum (Figure 5a). The addition of the peptide to the sample (0.2 mM increments, up to a final 2:1 molar ratio) resulted in many amide chemical shifts disappearing and re-appearing at different positions of the spectra. This observation of slow exchange on the NMR time scale is indicative of high affinity binding to the peptide. HNCACB and CBCACONH experiments were carried out for the reassignment of the backbone resonances of wPABC in a 1:1 complex with PAM-2. A comparison of amide signals obtained from ^{15}N-^{1}H HSQC spectra with and without the peptide displays residues M571 (0.427 ppm), E574 (0.711 ppm), Y577 (0.428 ppm), K590 (0.493 ppm), M594 (0.776 ppm), L595 (0.578 ppm), E619 (0.509 ppm), A620 (0.693 ppm), M621 (0.986 ppm), and V623 (0.447 ppm) having the largest change chemical shift changes upon binding (Figure 5b). They reside on helices α2, α3, and α5 and define the peptide binding pocket for wPABC (Figure 5d). wPABC binds peptides in a manner highly analogous to that of human and trypanosome PABC (*35*, *37*). The peptide binding residues are completely conserved throughout plant PABPs, indicating that all share a comparable peptide recognition mechanism (Figure 3).

Bioinformatic Survey of Plant PAM-2 Proteins. Recently, new plant PABP-interacting proteins were identified *in vivo* in both *Cucumis sativus* (*55*) and *Arabidopsis thaliana* (*56*). These proteins bind specifically to the PABC domain from PABP. Through primary sequence alignments, a PAM-2 site highly similar to the metazoan PAM-2 motif was identified (*55*). The PAM-2 sequence found in *A. thaliana* and *C. sativus* was used as a query to search the wheat genomic database. Eight distinct proteins were identified (Table 2), seven of which have homologues in other monocot (*T. aevestium*, *O. sativa*, and *C. sativus*) and dicot species (*N. tabacum* and *A. thaliana*). Aside from the early response to dehydration protein (ERD-15), the remaining proteins have not been characterized. However, all have conserved domains that give insight into their possible functions. The plant PAM-2 motif proteins can be divided into five categories on the basis of the presence of an acid-rich PAM-1-like region, RRM domains, SMR endonuclease domains, eIF3-like/tetratricopeptide repeats (TPR), or a Pbp1p/Lsm homology region (Figure 4).

There are two genes that contain an acid-rich PAM-1-like motif. The first is an early response to dehydration protein (ERD-15) (TC265113), which belongs to a class of genes activated in response to various stresses (*57*). For example, in *A. thaliana*, the ERD-15 expression level increases upon exposure to drought, low temperatures, and high light intensity (*58*). In *C. sativus*, a distinct diurnal pattern of PCI6/ERD gene expression was observed where transcript levels increased throughout the day and declined overnight (*55*). Homologues of this gene are found in both monocot and dicot species (Table 2) with high conservation in the first 60−65 residues (*55*, *57*). The N-terminal segment contains a PAM-2 motif, and site-directed mutagenesis studies confirmed that the motif was necessary for interacting

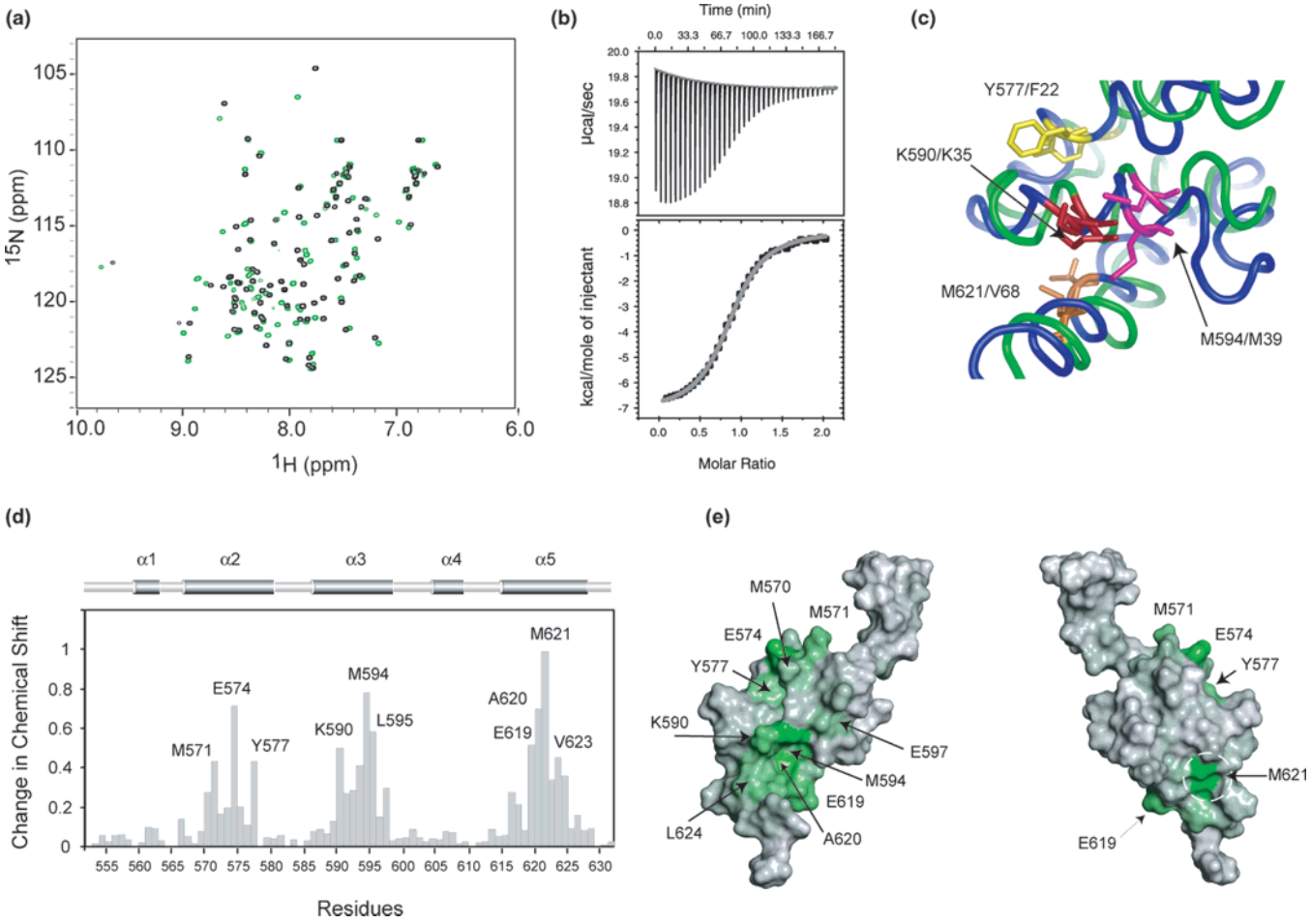

FIGURE 5: Peptide binding studies by NMR and ITC. (a) Overlay of wPABC ^{15}N-^{1}H HSQC from free (black) and peptide bound (green) forms. (b) Isothermal calorimetry profile of the PAM-2 peptide and wPABC. Each peak shown in the ITC thermogram represents an injection from the peptide. Below the thermogram is the integration of each peak fitted with a curve assuming a 1:1 binding model. The K_d was calculated to be 3 μM. (c) Backbone overlay of the wheat (PDB code 2DYD) and human (PDB code 1G9L) PABCs. The residues most important for peptide recognition are labeled in both structures. The numbering scheme for hPABC is in accordance with those of previous studies (*35*). (d) Chemical shift difference values, obtained from NMR titration experiments, plotted as a function of residue number. The residues most shifted by peptide binding are labeled. (e) Chemical shift difference values mapped on a surface rendering of the wPABC structure. The left surface map shows the front of the protein and displays the peptide binding pocket. The right surface map shows the back of the protein. The residues most shifted upon peptide binding are shown in green and are labeled.

with the C-terminal domain of PABP (*55*). Furthermore, ERD/PCI6 from *C. sativus* down-regulates translation through PABP interaction *in vitro* (*55*). Because the ERD-15 family has a short region of acidic residues, similar to the PAM-1 motif, following the conserved N-terminal region (TC265113, Figure 4), it is plausible that the mechanism of its effect on translation is similar to that of Paip-2 (*23*). The acidic PAM-1 region in Paip-2 is proposed to disrupt PABP's affinity for the poly (A)-tail (*32*). Another small wheat protein (TC238656) also contains both a PAM-2 motif followed by an Asp/Glu-rich stretch. However, this protein is distinct from ERD-15 and shares no sequence similarity with Paip-2.

Two PAM-2-containing RNA binding proteins (RNBP A and B) are found in wheat (TC246947 and TC266478) and other plant species (Table 2). Although these RNA binding proteins have yet to be fully characterized, a homologue in *A. thaliana* was shown to be expressed during embryogenesis and in growing organs, suggesting a role in plant development (*59*). This group of proteins consists of ~350 residues including a PAM-2 site at the N-terminal followed by two RNA recognition motifs. The two RRMs share the highest similarity (SMART 00360) to those found in the human U2 small nuclear ribonucleoprotein particle (sRNP) auxiliary factor (hU2AF) (*60*). U2AF associates with the 3′-site early in pre-mRNA splicing and recognizes additional splicing factors (*61*). The idea of PABP involvement in mRNA splicing is not surprising because yeast PABP associates with subunits of the cleavage factors IA (*5*, *6*). Cleavage factors also cooperate with splicing factors for polyadenylation control and couple splicing with polyadenylation (*62*). In addition, in mammalian cells, PABP associates with the poly (A)-tail of unspliced pre-mRNA and is suggested to be involved in pre-mRNA processing (*10*).

Wheat contains a 670 residue protein (TC247565) that shares significant similarity to the C-terminal region of a p135 subunit of eukaryotic initiation factor eIF3, which also contains TPR repeats. TPR is an antiparallel α-helical protein interaction domain present in a wide range of proteins involved in transcription, cell cycle control, protein folding, and protein transport (*63*). eIF3 binds to eIF4G and to the 40S ribosomal subunit to promote the binding of initiator methionyl-tRNA and mRNA (*64*). Recent studies show that PABP plays a direct role in ribosomal joining and increases its efficiency in initiation complex formation (*21*). Hence, a

Table 2: Plant Proteins Containing a PABC-Interacting Motif (PAM-2)

Entry[a]	Species[b]	Predicted Gene Product[c]	PAM-2 sequence[d]	Similarity to Wheat homologue[e]
TC265113	*T.aevestium*	ERD-15	SSLNPEAPLFIPAAFQ	-/- **(144)**
AAT72926	*O.sativa*	ERD-15	SSLNPDAPLFIPAAFR	164/ 60% (166)
AAM64638	*A.thaliana*	ERD-15	STLNPDAPLFIPAAVR	163/ 33% (163)
AAF75749	*L.esculentum*	ERD-15	STLNPNAPLFVPSFVR	156/ 31% (156)
AAV92296	*P.menziesii*	ERD-15	STLNPNAPLFIPLAYR	55/ 58% (134)
AAQ18141	*C.sativus*	ERD15/PCI6	SMLNPNAPLFVPMAYR	50/ 52% (141)
AAZ20289	*A.hypogaea]*	ERD-15	PTLNPNAPLYIPAAFR	43/ 60% **(124)**
TC246947	*T.aevestium*	RNABP-a	KKLNPSAEEFVPLSRR	349/100% (349)
BAD28276	*O.sativa*	RNABP-a	SKLNPRAQEFVPSSRR	310/ 66% (359)
AAA86641	*A.thaliana*	RNABP-a	SKLNPMAKEFIPPSLT	304/ 51% (336)
TC266478	*T.aevestium*	RNABP-b	SKLNPMAEEFVPPSLA	344/100% **(332)**
XP479783	*O.sativa*	RNABP-b	SKLNPMAEEFVPPSLA	231/ 71% (302)
NP174556	*A.thaliana*	RNABP-b	SKLNPMAEEFVPPSLN	295/ 65% (358)
TC247565	*T.aevestium*	TPR	PTMNPHAAEFVPGKTV	-/- (659)
CAE03171	*O.sativa*	TPR	PTMNPHAAEFVPGKTS	649/ 67% **(1720)**
NP172981	*A.thaliana*	TPR	RSMNPDAPEFVPRRSL	657/ 30% (1558)
TC251957	*T.aevestium*	SMRa	TSLNPNAVEFVPSCLR	-/- (567)
AAN65434	*O sativa*	SMRa	TALNPNAQEFVPSSLR	410/ 78% (581)
TC252881	*T.aevestium*	SMRb	TALNPNAAEFVPSCVI	-/- **(538)**
BAD35574	*O.sativa*	SMRb	TALNPNAAEFVPSCIR	427/ 79% (531)
AAC14523	*A.thaliana*	SMRb	TTLNPHAAEFVPFTLR	188/ 34% (567)
TC255400	*T.aevestium*	Lsm	SSLNPNAKEFKLNPNA	-/- **(355)**
XP465657	*O.sativa*	Lsm	SSLNPNAKEFKLNPNA	362/ 52% (591)
NP175819	*A.thaliana*	Lsm	STLNPNAKEFKLNPNA	374/ 27% (587)
TC238656	*T.aevestium*	Unknown	SKLNPHAKVFAPSFAS	-/- **(286)**

[a] Gene accession numbers are from the TIGR database (in bold) and NCBI. [b] *Triticum aevestium* (wheat), *Oryza sativa* (rice), *Arabisopsis thaliana* (thale cress), *Lycopersicon esculentum* (tomato), *Pseudotsuga menziesii* (Douglas fir), *Cumis sativus* (cucumber), *Arachis hypogaea* (peanut). [c] The abbreviations are as follows: early response to dehydration (ERD); PABC-interacting protein (PCI); RNA binding protein (RNABP); tetratricopeptide repeat (TPR); small MutS related (SMR), like Sm domain (Lsm). [d] Highlighted residues show the conservation within the PAM-2 sequences. [e] Length of segment with highest similarity, % similarity to wheat protein, and total size of the protein.

putative function of the PAM-2 motif in plant eIF3-like/TPR proteins is to modulate translation by interacting with PABP during translation initiation.

The fourth set of plant proteins (TC251957 and TC252881) contains an N-terminal PAM-2 motif followed by a C-terminal region simliar to that of the human BCL-3 binding protein (hBCL3-BP). Both proteins share in common a small MutS related domain (Smr). The Smr domain is an endonuclease conserved in bacterial MutS2 proteins and is involved in the DNA damage repair system (*65*). Similarly, the Smr domain in hBCL3-BP contains nicking endonuclease activity and is possibly involved in coupling transcription with DNA repair or recombination (*66*). However, the function of this domain has not been fully established in eukaryotes (*67*).

The final wheat protein (TC238656), found in rice and *A. thaliana*, contains a nucleic acid binding Sm-like motif (Lsm). Sm/Lsm proteins are a widespread protein family (*68*) that participate in mRNA related metabolic processes, such as pre-mRNA splicing (*69*), mRNA decapping and degradation (*70*), and small nucleolar RNP assembly (*71*). The Lsm motif is also found in two other PABP binding proteins: metazoan ataxin-2 (*72*) and yeast Pbp1p (*73*). Polyglutamine expansion in Ataxin-2 is responsible for the human disease spinocerebellar ataxia type 2 (*74*). This protein contains a PAM-2 motif, and recent work has confirmed the *in vivo* interaction between Ataxin-2 and PABP and its role in regulating translation (*72*). Yeast Pbp1p also interacts with the C-terminal domain of PABP but through binding to a region outside of the PABC domain. Pbp1p functions to prevent the association of PABP with poly (A)-nuclease and controls mRNA polyadenylation (*73*).

DISCUSSION

Typically, only one gene encoding PABP is found in single cell eukaryotes, whereas multiple copies are found in metazoans and plant species. Humans have three functional genes for cytosolic PABPs, whereas the dicot *Arabidopsis thaliana* contains eight (*75*). In *A. thaliana*, two of the eight PABP genes only encode four RRM domains. Another dicot, *N. tabacum*, has three expressed PABP genes but only one has four RRMs. The other two contain only one or two RRMs; all contain PABC domains. Although detailed expression data for PABP in the monocot *O. sativa* are not available, the number of PABP genes and tissue distribution and abundance follow the same pattern observed in *A. thaliana* (*75*). The additional genes for PABPs in plants are organ specific and were proposed to have evolved for specialized functions in translation or mRNA metabolism (*26*, *76*−*78*). Their unique functions are likely due to sequence differences in the RRM region.

In contrast, the region corresponding to the PABC of plant PABPs displays little primary sequence diversity, indicating a specific and conserved function. This includes PABPs from chloroplasts (*C. reinhardtii*), monocots (*O. sativa* and *T. aevestium*), dicots (*N. tabacum* and *A. thaliana*), and ferns (*A. philitidis*). In this article, we found that wheat PABC possesses a structure and peptide binding function very similar to those of the domain from human PABP (Figure 5c). Both recognize a very similar 15 residue sequence

(PAM-2 motif). From the conservation of key residues responsible for maintaining protein fold and peptide specificity identified from wheat, we predict that all plant PABCs will have similar functional characteristics. This is supported by recent work, which shows that PAB2 and PAB5 from *A. thaliana* interact *in vivo* with multiple proteins containing a PAM-2 sequence (*56*). Furthermore, other work has demonstrated that mutating key residues in the PAM-2 site of *C. sativus* proteins diminishes or abolishes its interaction with PABP (*55*). From an evolutionary point of view, this suggests that the structure and function of PABCs evolved prior to the divergence of plant and animal kingdoms and have generally remained preserved over time.

A notable exception is the PABC of PAB7 from *A. thaliana*, which has a histidine (H534) in place of the aromatic tyrosine (Y577, in wheat) (Figure 4). According to the human PABC−PAM2 complex and the wPABC structure reported here, the analogous residue F22 (Figure 5c) is the single most important factor contributing to peptide binding (*38*). Consequently, we predict that the affinity of *A. thaliana* PAB7 for the PAM-2 motif will be considerably reduced. This may have consequences for the regulation of PABP function in *A. thaliana*. Cross-complementation studies of *A. thaliana* PAB2, 3, and 5 with yeast PABP null mutants show that all can restore viability (*11*−*13*); however, similar experiments have not been performed with PAB7. The same studies also show that only certain functions of yeast PABP can be complimented. Only yeast PABC contains differences in structure and sequence specificity (*27*). Hence, the differences between the PABC from plants and yeast may be responsible for this partial complementation of *Arabidopsis* PABP in yeast.

Thus far, only a limited set of PABC-interacting proteins have been characterized *in vivo*. In yeast, the PAN3−PABC interaction in the nucleus is necessary for modifying the 3′ poly (A)-tail to a specific length, which is required for efficient mRNA export (*7*, *9*). The interactions between Paip-1, Paip-2, and RF3 have been well characterized in metazoans. Recent work has also verified the *in vivo* interaction between ataxin-2 (*74*) and the anti-proliferative protein Tob2 (*79*). Sequence homologues for the metazoan and yeast PABC binding proteins are currently not known in plant species. The only functional characterization of a plant PAM-2 protein is ERD/PCI6 from *C. sativus*, which down regulates PABP-dependent translation *in vitro* (*55*). Other evidence has provided support of PABC's importance in translation regulation in plants. For example, the zucchini mosaic potyvirus RNA dependent DNA polymerase (RdRp) directly targets the *C. sativus* PABC in PABP to modulate host translation to promote viral replication (*80*). Comparable strategies are also seen with viruses infecting mammalian systems. For instance, HIV (*81*) and Caliciviruses (*82*) both encode proteases that specifically separate the RRM regions from PABC to induce host translational shutoff. Together, these observations suggest that the regulatory effects of translation via PABC are conserved in both animal and plant species.

A bioinformatic review of the plant sequence database identifies several proteins containing PAM-2 sequences. These PABC-interacting proteins contain a diverse range of modules that implicate their function in translation or mRNA metabolic pathways. Furthermore, recent studies in *A. thaliana* show that these PAM-2 homologues are ubiquitously expressed and interact with PABP *in vivo* (*56*). Importantly, they are conserved throughout plant species, implying a significant role for these proteins. From previous biochemical data established in other species, we can propose that their function will be to regulate gene expression by affecting PABP-dependent mRNA or translation-related processes. Intriguingly, these plant PAM-2 proteins have no metazoan sequence homologues. This suggests that PABC binding proteins have evolved separately but have developed converging function in regulating PABP. Overall, our observations indicate that plants have evolved a distinct regulatory mechanism for PABP-dependent gene expression. Although hypothetical, these predictions serve as a basis for further experiments and provide insight into plant RNA metabolic and translational regulatory pathways.

ACKNOWLEDGMENT

We thank Dr. Tara Sprules for her assistance with the 800 MHz spectrometers at the Quebec/Eastern Canada High Field NMR Facility (http://valine.nmrlab.mcgill.ca).

REFERENCES

1. Mangus, D. A., Evans, M. C., and Jacobson, A. (2003) Poly(A)-binding proteins: multifunctional scaffolds for the post-transcriptional control of gene expression, *Genome Biol. 4*, 223.
2. Kuhn, U., and Wahle, E. (2004) Structure and function of poly(A) binding proteins, *Biochim. Biophys. Acta 1678*, 67−84.
3. Thakurta, A. G., Ho Yoon, J., and Dhar, R. (2002) Schizosaccharomyces pombe spPABP, a homologue of Saccharomyces cerevisiae Pab1p, is a non-essential, shuttling protein that facilitates mRNA export, *Yeast 19*, 803−810.
4. Afonina, E., Stauber, R., and Pavlakis, G. N. (1998) The human poly(A)-binding protein 1 shuttles between the nucleus and the cytoplasm, *J. Biol. Chem. 273*, 13015−13021.
5. Minvielle-Sebastia, L., Preker, P. J., Wiederkehr, T., Strahm, Y., and Keller, W. (1997) The major yeast poly(A)-binding protein is associated with cleavage factor IA and functions in premessenger RNA 3′-end formation, *Proc. Natl. Acad. Sci. U.S.A. 94*, 7897−7902.
6. Amrani, N., Minet, M., Le Gouar, M., Lacroute, F., and Wyers, F. (1997) Yeast Pab1 interacts with Rna15 and participates in the control of the poly(A) tail length in vitro, *Mol. Cell. Biol. 17*, 3694−3701.
7. Mangus, D. A., Evans, M. C., Agrin, N. S., Smith, M., Gongidi, P., and Jacobson, A. (2004) Positive and negative regulation of poly(A) nuclease, *Mol. Cell. Biol. 24*, 5521−5533.
8. Brune, C., Munchel, S. E., Fischer, N., Podtelejnikov, A. V., and Weis, K. (2005) Yeast poly(A)-binding protein Pab1 shuttles between the nucleus and the cytoplasm and functions in mRNA export, *RNA 11*, 517−531.
9. Dunn, E. F., Hammell, C. M., Hodge, C. A., and Cole, C. N. (2005) Yeast poly(A)-binding protein, Pab1, and PAN, a poly(A) nuclease complex recruited by Pab1, connect mRNA biogenesis to export, *Genes Dev. 19*, 90−103.
10. Hosoda, N., Lejeune, F., and Maquat, L. E. (2006) Evidence that poly(A) binding protein C1 binds nuclear pre-mRNA poly(A) tails, *Mol. Cell. Biol. 26*, 3085−3097.
11. Palanivelu, R., Belostotsky, D. A., and Meagher, R. B. (2000) Arabidopsis thaliana poly (A) binding protein 2 (PAB2) functions in yeast translational and mRNA decay processes, *Plant J. 22*, 187−198.
12. Chekanova, J. A., Shaw, R. J., and Belostotsky, D. A. (2001) Analysis of an essential requirement for the poly(A) binding protein function using cross-species complementation, *Curr. Biol. 11*, 1207−1214.
13. Belostotsky, D. A., and Meagher, R. B. (1996) A pollen-, ovule-, and early embryo-specific poly(A) binding protein from Arabidopsis complements essential functions in yeast, *Plant Cell 8*, 1261−1275.

14. Chekanova, J. A., and Belostotsky, D. A. (2003) Evidence that poly(A) binding protein has an evolutionarily conserved function in facilitating mRNA biogenesis and export, *RNA 9*, 1476−1490.
15. Browning, K. S. (1996) The plant translational apparatus, *Plant Mol. Biol. 32*, 107−144.
16. Tarun, S. Z., Jr., and Sachs, A. B. (1996) Association of the yeast poly(A) tail binding protein with translation initiation factor eIF-4G, *EMBO J. 15*, 7168−7177.
17. Bi, X., and Goss, D. J. (2000) Wheat germ poly(A)-binding protein increases the ATPase and the RNA helicase activity of translation initiation factors eIF4A, eIF4B, and eIF-iso4F, *J. Biol. Chem. 275*, 17740−17746.
18. Haghighat, A., and Sonenberg, N. (1997) eIF4G dramatically enhances the binding of eIF4E to the mRNA 5′-cap structure, *J. Biol. Chem. 272*, 21677−21680.
19. Le, H., Tanguay, R. L., Balasta, M. L., Wei, C. C., Browning, K. S., Metz, A. M., Goss, D. J., and Gallie, D. R. (1997) Translation initiation factors eIF-iso4G and eIF-4B interact with the poly-(A)-binding protein and increase its RNA binding activity, *J. Biol. Chem. 272*, 16247−16255.
20. Bushell, M., Wood, W., Carpenter, G., Pain, V. M., Morley, S. J., and Clemens, M. J. (2001) Disruption of the interaction of mammalian protein synthesis eukaryotic initiation factor 4B with the poly(A)-binding protein by caspase- and viral protease-mediated cleavages, *J. Biol. Chem. 276*, 23922−23928.
21. Kahvejian, A., Svitkin, Y. V., Sukarieh, R., M'Boutchou, M. N., and Sonenberg, N. (2005) Mammalian poly(A)-binding protein is a eukaryotic translation initiation factor, which acts via multiple mechanisms, *Genes Dev. 19*, 104−113.
22. Gallie, D. R. (1998) A tale of two termini: a functional interaction between the termini of an mRNA is a pre-requisite for efficient translation initiation, *Gene 216*, 1−11.
23. Kahvejian, A., Roy, G., and Sonenberg, N. (2001) The mRNA closed-loop model: the function of PABP and PABP-interacting proteins in mRNA translation, *Cold Spring Harb. Symp. Quant. Biol. 66*, 293−300.
24. Browning, K. S., Webster, C., Roberts, J. K., and Ravel, J. M. (1992) Identification of an isozyme form of protein synthesis initiation factor 4F in plants, *J. Biol. Chem. 267*, 10096−10100.
25. Gallie, D. R., and Browning, K. S. (2001) eIF4G functionally differs from eIFiso4G in promoting internal initiation, cap-independent translation, and translation of structured mRNAs, *J. Biol. Chem. 276*, 36951−36960.
26. Le, H., and Gallie, D. R. (2000) Sequence diversity and conservation of the poly(A)-binding protein in plants, *Plant Sci. 152*, 101−114.
27. Kozlov, G., Siddiqui, N., Coillet-Matillon, S., Trempe, J. F., Ekiel, I., Sprules, T., and Gehring, K. (2002) Solution structure of the orphan PABC domain from Saccharomyces cerevisiae poly(A)-binding protein, *J. Biol. Chem. 277*, 22822−22828.
28. Deo, R. C., Bonanno, J. B., Sonenberg, N., and Burley, S. K. (1999) Recognition of polyadenylate RNA by the poly(A)-binding protein, *Cell 98*, 835−845.
29. Imataka, H., Gradi, A., and Sonenberg, N. (1998) A newly identified N-terminal amino acid sequence of human eIF4G binds poly(A)-binding protein and functions in poly(A)-dependent translation, *EMBO J. 17*, 7480−7489.
30. Collier, B., Gorgoni, B., Loveridge, C., Cooke, H. J., and Gray, N. K. (2005) The DAZL family proteins are PABP-binding proteins that regulate translation in germ cells, *EMBO J. 24*, 2656−2666.
31. Roy, G., De Crescenzo, G., Khaleghpour, K., Kahvejian, A., O'Connor-McCourt, M., and Sonenberg, N. (2002) Paip1 interacts with poly(A) binding protein through two independent binding motifs, *Mol. Cell. Biol. 22*, 3769−3782.
32. Khaleghpour, K., Svitkin, Y. V., Craig, A. W., DeMaria, C. T., Deo, R. C., Burley, S. K., and Sonenberg, N. (2001) Translational repression by a novel partner of human poly(A) binding protein, Paip2, *Mol. Cell 7*, 205−216.
33. Craig, A. W., Haghighat, A., Yu, A. T., and Sonenberg, N. (1998) Interaction of polyadenylate-binding protein with the eIF4G homologue PAIP enhances translation, *Nature 392*, 520−523.
34. Uchida, N., Hoshino, S., Imataka, H., Sonenberg, N., and Katada, T. (2002) A novel role of the mammalian GSPT/eRF3 associating with poly(A)-binding protein in cap/poly(A)-dependent translation, *J. Biol. Chem. 277*, 50286−50292.
35. Kozlov, G., Trempe, J. F., Khaleghpour, K., Kahvejian, A., Ekiel, I., and Gehring, K. (2001) Structure and function of the C-terminal PABC domain of human poly(A)- binding protein, *Proc. Natl. Acad. Sci. U.S.A. 98*, 4409−4413.
36. Deo, R. C., Sonenberg, N., and Burley, S. K. (2001) X-ray structure of the human hyperplastic discs protein: an ortholog of the C-terminal domain of poly(A)-binding protein, *Proc. Natl. Acad. Sci. U.S.A. 98*, 4414−4419.
37. Siddiqui, N., Kozlov, G., D'Orso, I., Trempe, J. F., and Gehring, K. (2003) Solution structure of the C-terminal domain from poly-(A)-binding protein in Trypanosoma cruzi, *Protein Sci. 12*, 1925−1933.
38. Kozlov, G., De Crescenzo, G., Lim, N. S., Siddiqui, N., Fantus, D., Kahvejian, A., Trempe, J. F., Elias, D., Ekiel, I., Sonenberg, N., O'Connor-McCourt, M., and Gehring, K. (2004) Structural basis of ligand recognition by PABC, a highly specific peptide-binding domain found in poly(A)-binding protein and a HECT ubiquitin ligase, *EMBO J. 23*, 272−281.
39. Bax, A., and Grzesiek, S. (1993) Methodological advances in protein NMR, *Acc. Chem. Res. 26*, 131−138.
40. Delaglio, F., Grzesiek, S., Vuister, G. W., Zhu, G., Pfeifer, J., and Bax, A. (1995) NMRPipe: a multidimensional spectral processing system based on UNIX pipes, *J. Biomol. NMR 6*, 277−293.
41. Bartels, C., Xia, T., Billeter, M., Güntert, P., and K., W. (1995) The program XEASY for computer-supported NMR spectral analysis of biological macromolecules, *J. Biomol. NMR 6*, 1−10.
42. Grzesiek, S., Dobeli, H., Gentz, R., Garotta, G., Labhardt, A. M., and Bax, A. (1992) 1H, 13C, and 15N NMR backbone assignments and secondary structure of human interferon-gamma, *Biochemistry 31*, 8180−8190.
43. Constantine, K. L., Goldfarb, V., Wittekind, M., Friedrichs, M. S., Anthony, J., Ng, S. C., and Mueller, L. (1993) Aliphatic 1H and 13C resonance assignments for the 26-10 antibody VL domain derived from heteronuclear multidimensional NMR spectroscopy, *J. Biomol. NMR 3*, 41−54.
44. Farrow, N. A., Muhandiram, R., Singer, A. U., Pascal, S. M., Kay, C. M., Gish, G., Shoelson, S. E., Pawson, T., Forman-Kay, J. D., and Kay, L. E. (1994) Backbone dynamics of a free and phosphopeptide-complexed Src homology 2 domain studied by 15N NMR relaxation, *Biochemistry 33*, 5984−6003.
45. Brunger, A. T., Adams, P. D., Clore, G. M., DeLano, W. L., Gros, P., Grosse-Kunstleve, R. W., Jiang, J. S., Kuszewski, J., Nilges, M., Pannu, N. S., Read, R. J., Rice, L. M., Simonson, T., and Warren, G. L. (1998) Crystallography & NMR system: A new software suite for macromolecular structure determination, *Acta Crystallogr., Sect. D 54*, 905−921.
46. Nilges, M., Macias, M. J., O'Donoghue, S. I., and Oschkinat, H. (1997) Automated NOESY interpretation with ambiguous distance restraints: the refined NMR solution structure of the pleckstrin homology domain from beta-spectrin, *J. Mol. Biol. 269*, 408−422.
47. Wuthrich, K. (1989) The development of nuclear magnetic resonance spectroscopy as a technique for protein structure determination, *Acc. Chem. Res. 22*, 36−44.
48. Cornilescu, G., Delaglio, F., and Bax, A. (1999) Protein backbone angle restraints from searching a database for chemical shift and sequence homology, *J. Biomol. NMR 13*, 289−302.
49. Laskowski, R. A., Rullmannn, J. A., MacArthur, M. W., Kaptein, R., and Thornton, J. M. (1996) AQUA and PROCHECK-NMR: programs for checking the quality of protein structures solved by NMR, *J. Biomol. NMR 8*, 477−486.
50. McGinnis, S., and Madden, T. L. (2004) BLAST: at the core of a powerful and diverse set of sequence analysis tools, *Nucleic Acids Res. 32*, W20−W25.
51. Marchler-Bauer, A., Anderson, J. B., DeWeese-Scott, C., Fedorova, N. D., Geer, L. Y., He, S., Hurwitz, D. I., Jackson, J. D., Jacobs, A. R., Lanczycki, C. J., Liebert, C. A., Liu, C., Madej, T., Marchler, G. H., Mazumder, R., Nikolskaya, A. N., Panchenko, A. R., Rao, B. S., Shoemaker, B. A., Simonyan, V., Song, J. S., Thiessen, P. A., Vasudevan, S., Wang, Y., Yamashita, R. A., Yin, J. J., and Bryant, S. H. (2003) CDD: a curated Entrez database of conserved domain alignments, *Nucleic Acids Res. 31*, 383−387.
52. Letunic, I., Copley, R. R., Schmidt, S., Ciccarelli, F. D., Doerks, T., Schultz, J., Ponting, C. P., and Bork, P. (2004) SMART 4.0: towards genomic data integration, *Nucleic Acids Res 32*, D142−D144.
53. Chenna, R., Sugawara, H., Koike, T., Lopez, R., Gibson, T. J., Higgins, D. G., and Thompson, J. D. (2003) Multiple sequence

alignment with the Clustal series of programs, *Nucleic Acids Res. 31*, 3497−3500.
54. Hoshino, S., Hosoda, N., Araki, Y., Kobayashi, T., Uchida, N., Funakoshi, Y., and Katada, T. (1999) Novel function of the eukaryotic polypeptide-chain releasing factor 3 (eRF3/GSPT) in the mRNA degradation pathway, *Biochemistry (Moscow, Russ. Ed.) 64*, 1367−1372.
55. Wang, X., and Grumet, R. (2004) Identification and characterization of proteins that interact with the carboxy terminus of poly-(A)-binding protein and inhibit translation in vitro, *Plant Mol. Biol. 54*, 85−98.
56. Bravo, J., Aguilar-Henonin, L., Olmedo, G., and Guzman, P. (2005) Four distinct classes of proteins as interaction partners of the PABC domain of Arabidopsis thaliana poly(A)-binding proteins, *Mol. Genet. Genomics 272*, 651−665.
57. Kiyosue, T., Yamaguchi-Shinozaki, K., and Shinozaki, K. (1994) ERD15, a cDNA for a dehydration-induced gene from Arabidopsis thaliana, *Plant Physiol. 106*, 1707.
58. Dunaeva, M., and Adamska, I. (2001) Identification of genes expressed in response to light stress in leaves of Arabidopsis thaliana using RNA differential display, *Eur. J. Biochem. 268*, 5521−5529.
59. Hecht, V., Stiefel, V., Delseny, M., and Gallois, P. (1997) A new Arabidopsis nucleic-acid-binding protein gene is highly expressed in dividing cells during development, *Plant Mol. Biol. 34*, 119−124.
60. Ito, T., Muto, Y., Green, M. R., and Yokoyama, S. (1999) Solution structures of the first and second RNA-binding domains of human U2 small nuclear ribonucleoprotein particle auxiliary factor (U2AF(65)), *EMBO J. 18*, 4523−4534.
61. Kielkopf, C. L., Rodionova, N. A., Green, M. R., and Burley, S. K. (2001) A novel peptide recognition mode revealed by the X-ray structure of a core U2AF35/U2AF65 heterodimer, *Cell 106*, 595−605.
62. Awasthi, S., and Alwine, J. C. (2003) Association of polyadenylation cleavage factor I with U1 snRNP, *RNA 9*, 1400−1409.
63. D'Andrea, L. D., and Regan, L. (2003) TPR proteins: the versatile helix, *Trends Biochem. Sci. 28*, 655−662.
64. Vornlocher, H. P., Hanachi, P., Ribeiro, S., and Hershey, J. W. (1999) A 110-kilodalton subunit of translation initiation factor eIF3 and an associated 135-kilodalton protein are encoded by the Saccharomyces cerevisiae TIF32 and TIF31 genes, *J. Biol. Chem. 274*, 16802−16812.
65. Moreira, D., and Philippe, H. (1999) Smr: a bacterial and eukaryotic homologue of the C-terminal region of the MutS2 family, *Trends Biochem. Sci. 24*, 298−300.
66. Murillas, R., Simms, K. S., Hatakeyama, S., Weissman, A. M., and Kuehn, M. R. (2002) Identification of developmentally expressed proteins that functionally interact with Nedd4 ubiquitin ligase, *J. Biol. Chem. 277*, 2897−2907.
67. Malik, H. S., and Henikoff, S. (2000) Dual recognition-incision enzymes might be involved in mismatch repair and meiosis, *Trends Biochem. Sci. 25*, 414−418.
68. Anantharaman, V., and Aravind, L. (2004) Novel conserved domains in proteins with predicted roles in eukaryotic cell-cycle regulation, decapping and RNA stability, *BMC Genomics 5*, 45.
69. Will, C. L., and Luhrmann, R. (2001) Spliceosomal UsnRNP biogenesis, structure and function, *Curr. Opin. Cell. Biol. 13*, 290−301.
70. Tharun, S., and Parker, R. (2001) Targeting an mRNA for decapping: displacement of translation factors and association of the Lsm1p-7p complex on deadenylated yeast mRNAs, *Mol. Cell 8*, 1075−1083.
71. Kufel, J., Allmang, C., Petfalski, E., Beggs, J., and Tollervey, D. (2003) Lsm Proteins are required for normal processing and stability of ribosomal RNAs, *J. Biol. Chem. 278*, 2147−2156.
72. Ciosk, R., DePalma, M., and Priess, J. R. (2004) ATX-2, the C. elegans ortholog of ataxin 2, functions in translational regulation in the germline, *Development 131*, 4831−4841.
73. Mangus, D. A., Amrani, N., and Jacobson, A. (1998) Pbp1p, a factor interacting with Saccharomyces cerevisiae poly(A)-binding protein, regulates polyadenylation, *Mol. Cell. Biol. 18*, 7383−7396.
74. Ralser, M., Albrecht, M., Nonhoff, U., Lengauer, T., Lehrach, H., and Krobitsch, S. (2005) An integrative approach to gain insights into the cellular function of human ataxin-2, *J. Mol. Biol. 346*, 203−214.
75. Belostotsky, D. A. (2003) Unexpected complexity of poly(A)-binding protein gene families in flowering plants: three conserved lineages that are at least 200 million years old and possible auto- and cross-regulation, *Genetics 163*, 311−319.
76. Feral, C., Guellaen, G., and Pawlak, A. (2001) Human testis expresses a specific poly(A)-binding protein, *Nucleic Acids Res. 29*, 1872−1883.
77. Yang, H., Duckett, C. S., and Lindsten, T. (1995) iPABP, an inducible poly(A)-binding protein detected in activated human T cells, *Mol. Cell. Biol. 15*, 6770−6776.
78. Belostotsky, D. A., and Meagher, R. B. (1993) Differential organ-specific expression of three poly(A)-binding-protein genes from Arabidopsis thaliana, *Proc. Natl. Acad. Sci. U.S.A. 90*, 6686−6690.
79. Okochi, K., Suzuki, T., Inoue, J., Matsuda, S., and Yamamoto, T. (2005) Interaction of anti-proliferative protein Tob with poly(A)-binding protein and inducible poly(A)-binding protein: implication of Tob in translational control, *Genes Cells 10*, 151−163.
80. Wang, X., Ullah, Z., and Grumet, R. (2000) Interaction between zucchini yellow mosaic potyvirus RNA-dependent RNA polymerase and host poly-(A) binding protein, *Virology 275*, 433−443.
81. Alvarez, E., Castello, A., Menendez-Arias, L., and Carrasco, L. (2006) HIV protease cleaves poly(A) binding protein, *Biochem. J. 396*, 219−226.
82. Kuyumcu-Martinez, M., Belliot, G., Sosnovtsev, S. V., Chang, K. O., Green, K. Y., and Lloyd, R. E. (2004) Calicivirus 3C-like proteinase inhibits cellular translation by cleavage of poly(A)-binding protein, *J. Virol. 78*, 8172−8182.

BI061986D